LWT - Food Science and Technology 147 (2021) 111643

Contents lists available at ScienceDirect

LWT

journal homepage: www.elsevier.com/locate/lwt

Rheological properties of xanthan-modified fish gelatin and its potential to replace mammalian gelatin in low-fat stirred yogurt

Mengdi Yin [a,b], Dongying Yang [a], Shaojuan Lai [c,d,*], Hongshun Yang [a,b,**]

[a] Department of Food Science and Technology, National University of Singapore, 117542, Singapore
[b] National University of Singapore (Suzhou) Research Institute, 377 Lin Quan Street, Suzhou Industrial Park, Suzhou, Jiangsu 215123, PR China
[c] College of Basic Medicine, Guizhou University of Traditional Chinese Medicine, Guiyang, Guizhou 550025, PR China
[d] College of Food Science and Technology, Henan University of Technology, Zhengzhou, Henan 450001, PR China

ARTICLE INFO

Keywords:
Fish gelatin
Porcine gelatin
Polysaccharide
Dairy product
Rheology

ABSTRACT

Fish gelatin (FG) has been modified to replace mammalian gelatin, but has not been applied in the yogurt production. In this study, xanthan gum (XG) was used to improve the rheology properties of FG, and the XG-modified FG was applied in acid milk gels and low-fat yogurts to mimic the rheology and texture properties of porcine gelatin (PG). No obvious difference in the storage moduli was observed for the FG gels (2.5 g/100 g) with the addition of XG from 0 to 0.05 g/100 g, while increasing addition of XG increasingly impeded the gelation process of FG. Moreover, in the milk gel system with FG addition (0.4 g/100 g), an increase in the XG proportion caused an increase in the storage moduli. Milk gels with a XG to FG ratio of 1:99 best mimicked the storage moduli of milk gels with PG. In the yogurt system, yogurt with 0.4 g/100 g XG-modified FG had better water-holding capacity and consistency than the yogurt with 0.4 g/100 g PG, and had similar viscosity, pseudoplasticity, and thixotropy to yogurt with 0.4 g/100 g PG. The results suggested that XG-modified FG is a promising replacement for mammalian gelatin in low-fat stirred yogurt.

1. Introduction

Low-fat yogurt is a popular consumed milk product with an increasing market demand because of the trend for low-calorie diets around the world. Typically, the taste of low-fat yogurt is not as good as whole-fat yogurt because fat reduction can cause defects such as lack of flavor, weak body, and poor texture (Nguyen, Kravchuk, Bhandari, & Prakash, 2017). Gelatin is one of the most popular fat replacers, which can improve the rigidity and stability of low-fat yogurt. The unique property of gelatin is its 'melt in the mouth' feeling, which provides a fat-like sensory perception to low-fat yogurt (Karim & Bhat, 2009).

At present, most commercial gelatin is derived from porcine and bovine (Sha et al., 2018). However, gelatin originating from mammals has the potential of spreading bovine spongiform encephalopathy (BSE), foot-and-mouth disease (FMD), and avian influenza. Moreover, products made with mammalian gelatin are not acceptable for consumer groups with certain religious beliefs, such as Jews and Muslims (Kamer et al., 2019). Therefore, fish gelatin (FG) has been studied as a potential alternative to mammalian gelatin in the food industry in recent years (Sow, Chong, Liao, & Yang, 2018; Sow, Toh, Wong, & Yang, 2019; Sow & Yang, 2015).

FG is a high molecular polypeptide polymer. It is partially hydrolyzed from fish collagen, which can be easily obtained from fish skin, scale, and bone. The production of FG helps to utilize waste materials in the fish industry. In general, FG has different rheology properties to those of mammalian gelatin, such as gel strength, as a result of its lower content of proline (Pro) and hydroxyproline (Hyp) (Jellouli et al., 2011). Pang, Deeth, Yang, Prakash, and Bansal (2017) studied the rheological performance of FG and bovine gelatin (BG) in acid milk gel and yogurt systems, and found detectable differences in rheological and texture properties. Sodium alginate and low acyl gellan have been used to modify and improve the rheology properties of FG; however, no research has applied modified FG in a yogurt system and evaluated its performance.

Xanthan gum (XG) is an anionic polysaccharide produced from *Xanthomonas campestris* (Chivero, Gohtani, Yoshii, & Nakamura, 2015). Cations can connect with XG molecules to form salt bridges and promote the formation of a double helix structure (Wu et al., 2019). Tilapia skin

* Corresponding author. College of Basic Medicine, Guizhou University of Traditional Chinese Medicine, Guiyang, Guizhou 550025, PR China.
** Corresponding author. Department of Food Science and Technology, National University of Singapore, 117542, Singapore.
E-mail addresses: shaojuanlai@hotmail.com (S. Lai), fstynghs@nus.edu.sg (H. Yang).

https://doi.org/10.1016/j.lwt.2021.111643
Received 12 March 2021; Received in revised form 22 April 2021; Accepted 1 May 2021
Available online 7 May 2021

gelatin (the FG type used in this study) is positively charged at a pH lower than its isoelectric point (pI) (da Trindade Alfaro, Fonseca, & Prentice-Hernández, 2013). Therefore, the electrical interaction between FG and XG might promote the formation of the double helix structure in XG. Furthermore, Laneuville, Turgeon, Sanchez, and Paquin (2006) reported that natural β-lactoglobulin and XG are synergistic for gelling at a low concentration (0.1 g/100 g); and Pang, Deeth, Sharma, and Bansal (2015) observed a marked increase in the storage moduli (G′) of milk gel with 0.01 g/100 g XG addition.

The aim of this study was to evaluate the rheological properties of xanthan gum-modified fish gelatin (XG-FG) in pure solutions and in acid milk gels. Moreover, the quality of low-fat yogurts with the addition of FG, XG-FG, and PG was compared. The results will contribute to the future application of polysaccharide-modified fish gelatin to replace mammalian gelatin in low-fat yogurt.

2. Materials and methods

2.1. Materials

Commercial tilapia FG (240 Bloom) and PG (240 Bloom) were purchased from Chengdu Jingdian Co. Ltd. (Sichuan, China). Xanthan gum (Sigma®, 11138-66-2) and Glucono-δ-lactone (Sigma®, G4750) were purchased from Sigma-Aldrich Co. Ltd (Singapore). Skim milk powder (SMP; protein 32.3, moisture 3.9, fat 0.9, lactose 53.7, and ash 9.2 g/100 g) was purchased from Cowhead Ltd. (Singapore). The yogurt starter (Chr. Hansen®, YC-380, *Streptococcus thermophilus* and *Lactobacillus delbrueckii* ssp. bulgaricus, Chr. Hansen) was obtained from Chr. Hansen Co. Ltd (Singapore).

2.2. Sample preparation

2.2.1. The XG-FG mixture

The samples were prepared according to the method of Wang, Natale, Virgilio, and Heuzey (2016) with some modifications. FG and XG solutions were held in deionized water for 10 h and then heated for 10 min at 65 °C with stirring. Afterwards, the solutions were blended and heated for 30 min at 60 °C to reach an overall concentration of 2.5 g/100 g and ratios of XG to FG (w/w) of 0:100, 0.5:99.5, 1:99, 1.5:98.5, and 2:98, as shown in Table S1. All prepared solutions had a pH between 6.2 and 6.4.

2.2.2. XG-FG acid milk gel and PG acid milk gel

Reconstituted milk with 4.5 g/100 g milk protein was obtained by dispersing the SMP in deionized water with constant stirring for 30 min. Then, PG solutions and XG-FG solutions with ratios of XG to FG (w/w) of 0:100, 1:99, and 1.5:99.5 were added to the milk to achieve an overall concentration of 0.4 g/100 g. The samples were kept at 4 °C for 10 h before use. Afterwards, the samples were heated at 95 °C for 10 min at their natural pH, followed by cooling down to 45 °C. Glucono-δ-lactone (1.5 g/100 g) was mixed into all samples to decrease pH to 4.6 after 4 h at 45 °C.

2.2.3. Yogurt

An XG-FG solution with a ratio of XG to FG of 1:99 (w/w) was added to the reconstituted milk (total solids 13.4, protein 4.5, fat 0.1, and ash 1.3 g/100 g) to achieve an XG-FG concentration of 0.4 g/100 g. The same concentrations were studied for PG. Then, the mixtures were heated to 95 °C for 10 min and cooled to 42 °C immediately. And then the yogurt starter was inoculated into the mixtures at a concentration of 0.2 U/kg, and mixtures were incubated at 42 °C for 6 h until the pH reached 4.6. The yogurts were then cooled rapidly for storage at 4 °C for 48 h until evaluation.

2.3. Zeta potential

The samples were diluted with deionized water to 0.01 g/100 g, followed by cooling down to 25 °C. Zeta potential (ζ-) measurements were performed by a NanoBrook Omni Particle Size and Zeta Potential analyzer (Brookhaven Instruments, Holtsville, NY, USA) with phase analysis light scattering mode and Smoluchowski's model. (Sow et al., 2018).

2.4. Rheological tests

2.4.1. XG-FG gel

Gelatin gels (2.5 g/100 g) were used for dynamic oscillatory measurements by Anton Paar MCR 102 stress-controlled rheometer (Anton Paar, Graz, Austria). Test samples were placed onto the rheometer plate at 30 °C. The geometry used was a steel cone plate (angle: 1°, diameter: 60 mm, 0.1667 mm gap). Before the experiments, a strain sweep indicated that 0.5 g/100 g strain at a frequency of 1 Hz fell in the linear viscoelastic region for all samples. The experiments were conducted in three stages: comprising cooling, annealing, and heating, as defined by Pang, Deeth, Sharma, and Bansal (2015):

(1) Cooling: The rheometer was equilibrated at 30 °C and then cooled down to 10 °C at a speed of 1 °C/min in order to form gelatin gel;
(2) Annealing: A time sweep (10 °C, 1 h) in order to record the maturation process of the gel;
(3) Heating: A temperature sweep (10–30 °C) at a speed of 1 °C/min to record the melting of the gel, which relates to the "melt-in-mouth" feeling of gelatin in yogurt.

The gelling and melting behavior were observed as complex viscosity (η*) significantly increases and decreases, respectively. The complex viscosity, η*, was described in Eq. (1):

$$\eta * = x = \sqrt{G'^2 + G''^2}/\omega \quad (1)$$

where G′ is the storage modulus; G″ is the loss modulus; and ω is the frequency.

2.4.2. XG-FG acid milk gel and PG acid milk gel

Test samples were loaded at 45 °C onto the stress-controlled rheometer and measurement parameters were the same as those described in section 2.3.1. The samples remained were immediately placed in a water bath at 45 °C for acidification. After 4 h (at pH 4.6), the samples were stirred at 1200 rpm for 2 min and stored at 10 °C in an incubator. Dynamic oscillatory measurements were conducted in four stages (acidification, cooling, annealing, and heating) as defined by Pang, Deeth, Sharma, and Bansal (2015):

(1) Acidification: The samples were kept at 45 °C for 4 h to achieve pH 4.6;
(2) Cooling: A temperature sweep to 10 °C at a speed of 1 °C/min in order to form gel;
(3) Annealing: Maintained at 10 °C for 2.5 h in order to record the maturation process of the gel;
(4) Heating: A temperature sweep to 45 °C at a speed of 1 °C/min in order to record the melting process of the samples.

Pre-experiments showed that a strain of 0.5 g/100 g at a frequency of 1 Hz fell in the linear viscoelastic region of the samples (Pang, Deeth, & Bansal, 2015).

2.4.3. Yogurt

Yogurt samples were loaded at 10 °C onto the same stress-controlled rheometer as described in sections 2.3.1 and 2.3.2. Shear stress was recorded with shear rate changing from 0 to 100 s^{-1} (upward flow

curve) and followed by 100 to 0 s^{-1} (downward flow curve). Afterwards, the upward flow curve was fitted to the Hershel-Bulkley model (Eq. (2)) (Luo, Liu, & Pang, 2019):

$$\sigma = \sigma_0 + K\ \dot{\gamma}^n \quad (2)$$

where σ is the shear stress; σ_0 is the yield stress; K is the consistency index; $\dot{\gamma}$ is the shear rate; and n is the flow behavior index. The area under the upward flow curve (A_{up}) and the difference in the area under the two curves (ΔA) were also obtained.

Moreover, the frequency was increased from 0.01 to 10 Hz to carry out a frequency sweep to evaluate the viscoelastic properties of the yogurt. The applied strain was 0.5 g/100 g, which fell in the linear viscoelastic range. The G′ and G″ were obtained to calculate loss tangent. Afterwards, the slopes of the log-log plots for G′ and G″ were calculated.

2.5. Texture analysis

The textural properties of yogurt were measured using a TA-XT2i texture analyzer (Stable Micro System Ltd., Godalming, UK). Samples after acidification, as prepared in section 2.3.3, were kept at 10 °C for 48 h before measurement. The textural properties of yogurt were measured according to the method of Pang, Deeth, Sharma, and Bansal (2015) with some modifications. The probe was cylindrical, with a flat base of 20 mm in diameter. The sample was contained in a cylindrical container of 50 mm in diameter at 75% full. The parameters were set as: Test speed = 1 mm/s, compression depth = 10 mm. Firmness (g), consistency (g·s), and cohesiveness (g) were quantified.

2.6. Water-holding capacity

The water-holding capacity (WHC) was measured according to Pang, Deeth, and Bansal (2015) with some modifications. Yogurt was centrifuged at 400×*g* at 10 °C for 10 min. WHC was defined as follows:

$$\text{WHC}\ (\%) = 100(\text{Y weight} - \text{SE weight})/\ \text{Y weight}$$

Where Y is yogurt; SE is serum expelled.

2.7. Sensory evaluation

The sensory evaluation was approved by the NUS Institutional Review Board (NUS-IRB). The reference code is NUS-IRB-2020-576. The sensory evaluation was performed using the quantitative descriptive analysis (QDA) method, according to Kaur, Kumar, and Dhaliwal (2020). Sensory evaluation was conducted by a trained panel of 6 males and 6 females varying from 20 to 40 years old. In the examined yogurt samples, 5 individual quality features were taken into account, including sense of melting, homogeneity, thickness, stickiness, and aroma. The descriptors describing the characteristics of the tested samples along with their definitions were decided by the panel after training, and are shown in Table S2. The panelists scored quality characteristics of each sample on a 7-point rating scale. The score of 6 indicated an "extremely strong" degree, while the score of 0 represented a "very weak" degree.

2.8. Microstructure

The microstructure was studied according to the method described by Dai, Corke, and Shah (2016) with slight modifications. The samples were stored at 10 °C for 48 h before observation. To stain the yogurt samples, Rhodamine B and fluorescein isothiocyanate (FITC) were used to label FG and XG, respectively. Twenty microliters of Rhodamine B (1 mg/mL in dimethyl sulfoxide (DMSO)) and 20 μL of FITC (1 mg/mL in DMSO) were mixed with a 1-mL yogurt sample for 30 min. The excitation/emission wavelengths for FITC and rhodamine B were 495/525 nm and 543/580 nm, respectively. Thereafter, 50 μL of the stained sample was pipetted onto a glass slide and sealed with a coverslip. The microstructure was captured using confocal laser scanning microscopy (CLSM) with an Olympus Fluoview FV 1000 confocal scanning unit (Tokyo, Japan) embedded with argon ion and HeliumNeon (HeNe) lasers. Images were captured at 60× magnification with water immersion. Afterwards, images were annotated by Fluoview Software (Olympus).

2.9. Statistical analysis

All tests were performed in triplicate, independently, and the results were expressed as the mean ± standard deviation. SPSS Statistics 20 software (IBM Corp., Armonk, NY, USA) was used for analysis of variance (ANOVA) ($P < 0.05$) testing.

3. Results and discussion

3.1. Effects of XG on the zeta potential of FG

The effects of XG addition on the zeta potential of the FG solution are shown in Table 1. XG was strongly negatively charged (−54.19 ± 1.80 mV) while FG was weakly positive (10.33 ± 0.98 mV). The XG-FG mixtures showed a slight decrease in zeta potential as the XG ratio increased. The results were consistent with the report of Wang et al. (2016), who reported a decrease in the zeta potential of FG with the addition of XG caused by the electrostatic interaction. As the XG:FG (w/w) increased to 2:98, the zeta potential remained positive (7.33 ± 0.54 mV), indicating that the positively charged FG was not fully bound by XG.

3.2. Effects of XG on the rheological properties of FG gels, acid milk gels, and yogurt

3.2.1. XG-FG gel

Preliminary data showed that 2.5 g/100 g was the minimal gelling concentration for pure FG solution, which agreed with the data from Pang, Deeth, Sopade, Sharma, and Bansal (2014, 2017). During the three stages (cooling, annealing, and heating), the representative changes in G′ and G″ for the XG-FG mixtures at a concentration of 2.5 g/100 g are shown in Fig. 1A–C. The mean values of G′ at the end of each stage are shown in Table 1.

During cooling, the intersection point of G′ and G″ indicates the gelling point (Andersen, Ibsen, & Birkedal, 2018). From Fig. 1A, the pure FG solution had obvious gelling point (14 °C), which was similar to the values reported by Pang et al. (2014). With the addition of XG, the intersection point disappeared, even at a level as low as 0.5 g/100 g. Without an intersection point, gelling behavior can be inferred at the point where an appreciable decrease in complex viscosity (η*) appeared (Jellouli et al., 2011; Sopade, Halley, & Junming, 2004). Fig. 1D shows the change of η* of XG-FG mixtures in the cooling stage. From Fig. 1D, the upward curve of η*, as a result of temperature reduction, became

Table 1
Zeta potential and storage modulus (G′) of the xanthan gum (XG)-fish gelatin (FG) mixtures at the end of each stage. Values are presented as the mean ± SD.

Sample name	Zeta Potential (mV)	Storage modulus at the end of each stage (Pa)		
		Cooling	Annealing	Heating
FX0	10.33 ± 0.98^{a}	49.6 ± 1.2^{ab}	370.5 ± 18.9^{a}	0.1 ± 0.0^{c}
FX0.5	10.18 ± 0.51^{a}	34.6 ± 0.7^{b}	325.4 ± 3.8^{a}	0.3 ± 0.2^{c}
FX1	9.18 ± 0.31^{ab}	36.2 ± 13.7^{b}	320.8 ± 36.0^{a}	0.5 ± 0.0^{c}
FX1.5	8.26 ± 0.7^{b}	34.6 ± 14.8^{b}	326.2 ± 11.2^{a}	1.5 ± 0.5^{b}
FX2	7.33 ± 0.46^{bc}	74.6 ± 3.0^{a}	385.7 ± 1.0^{a}	3.5 ± 0.0^{a}

[a-c] Mean values within a column and within a gel type with different letters are significantly different ($P < 0.05$).
*FX0, FX0.5, FX1, FX1.5, and FX2 refer to the samples with proportions of xanthan gum to fish gelatin of 0:100.0.5:99.5, 1:99, 1.5:98.5, and 2:98 (w/w), respectively.

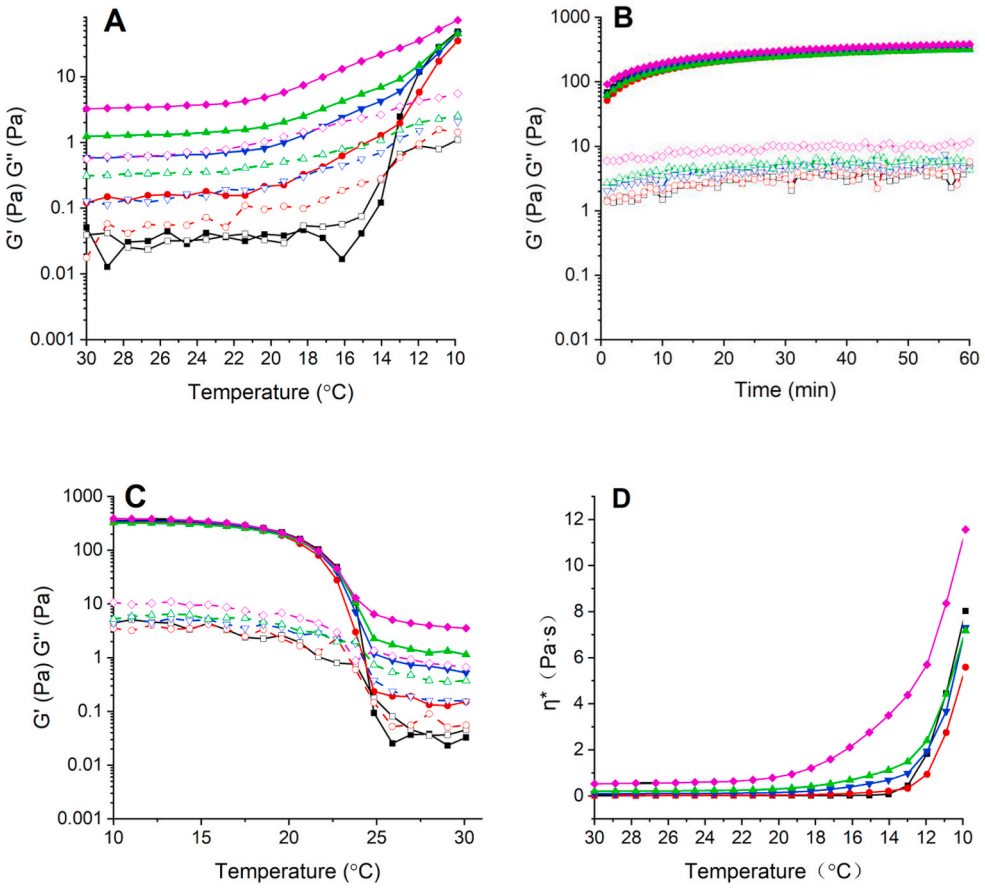

Fig. 1. Changes in the storage modulus (G′) and loss modulus (G″) in a xanthan gum-fish gelatin mixture (A: Cooling from 45 to 10 °C; B: annealing at 10 °C; C: heating from 10 to 30 °C.). Xanthan gum and fish gelatin were set at ratios of 0:100 (FX0), 0.5:99.5 (FX0.5), 1:99 (FX1), 1.5:98.5 (FX1.5), 2:98 (FX2). ■, G′ of FX0; □, G″ of FX0; ●, G′ of FX0.5; ○, G″ of FX0; ▼, G′ of FX1; ▽, G″ of FX0; ▲, G′ of FX1.5; △, G″ of FX0; ◆, G′ of FX2; ◇, G″ of FX0. (D): Changes in Complex Viscosity (η*) when the temperature changed from 30 to 10 °C. Xanthan gum and fish gelatin were set at ratios of 0:100 (■, FX0), 0.5:99.5 (●, FX0.5), 1:99 (▼, FX1), 1.5:98.5 (▲, FX1.5), 2:98 (◆, FX2).

smoother with increasing XG concentration. FX0.5, FX1, and FX1.5 showed gelling behavior (a sudden increase in the slope of the curve) within the range of 13–14 °C, which was similar to the pure FG solution (FX0). However, the curve of FX2 had no inflection point, and a steady increase in η* was observed. This result indicated that the addition of XG slowed down the gelling process of FG. Therefore, the ratio of XG to FG of 2:98 was not used in subsequent experiments because of the apparent impediment on the gelation process of FG. In addition, the ratio of XG to FG of 0.5:99.5 was also eliminated form following experiments because of its similar η* to the pure FG solution.

During annealing, the rheograms were fitted to a modified first-order kinetic model (Eq. (3) in Pang et al., 2014). Within the time range, regression analysis indicated that the first-order kinetic model showed prominent correlation coefficients ($P < 0.05$), revealing that this model is appropriate to describe the result data in our research:

$$G_t' = G_0' + G_{\infty-0}' [1 - exp(-kt)], \quad (3)$$

$$G_\infty' = G_0' + G_{\infty-0}' \quad (4)$$

where G_0' is G′ at time t = 0; G_∞′ is G′ at infinite time (t → ∞); and k is the rate of gelation during annealing. The average gelation rate K of FX0, FX0.5, FX1, FX1.5, and FX2 were calculated as 3.65×10^{-2}, 3.57×10^{-2}, 3.56×10^{-2}, 3.61×10^{-2}, and 3.74×10^{-2} respectively, with no significant difference ($P > 0.05$). This indicated that XG within this concentration range had no obvious impact on the maturation process of the FG gel. At the end of the annealing stage, no noticeable difference in G′ was observed in samples with various concentrations of XG ($P > 0.05$). The observation in our study might be caused by the low partition of XG in FG, which led to an unnoticeable effect on the G′ value of the gel system.

Based on the zeta potential and rheological test, Fig. 2 illustrates the gelling parameters of the XG-FG gel. Electrostatic interaction between the negatively charged pyruvate group of XG (Bergmann, Furth, & Mayer, 2008) and the positively charged amino group residues of FG (Derkach, Voron'ko, Maklakova, & Kondratyuk, 2014) is also illustrated. FG has an ordered helix structure reinforced by hydrogen bonds below the melting point and a coil structure above this point (Huang et al., 2017); XG has an ordered double helix structure because of noncovalent bonds (such as intermolecular hydrogen bonds) below the transition temperature (T_m, 52 °C), and a disordered curling chain structure above the T_m (Milas, Reed, & Printz, 1996; Pelletier, Viebke, Meadows, & Williams, 2001). Thus, XG remained in the helix structure during the whole experimental process.

At the end of the heating stage, the G′ value of the XG-FG mixtures increased significantly with increasing XG concentration ($P < 0.05$; Table 1). At this point, the helix structure of FG broke down, while XG still existed in a helix form. Therefore, the rigidity of the system might be primarily affected by XG, which could explain the obvious difference in the G′ value among samples with different XG concentrations.

3.2.2. XG-FG acid milk gel and PG acid milk gel

The G′ value at the end of each stage improved significantly with increasing XG concentration ($P < 0.05$, Table 2). The acid milk gel with an XG:FG ratio of 1:99 could best mimic the G′ value of the acid milk gel with PG during the four stages (Table 2). Electrostatic interactions between XG and milk casein could form between the negatively charged pyruvate group of XG (Bergmann et al., 2008) and positively charged amino acid residues (Glu and Asp) in κ-casein surrounding the milk casein (Creamer, Plowman, Liddell, Smith, & Hill, 1998). Thus, this electrostatic interaction between XG and milk proteins might have contributed to the increase in the G′ value. Lucey, Van, Grolle, Geurts, &

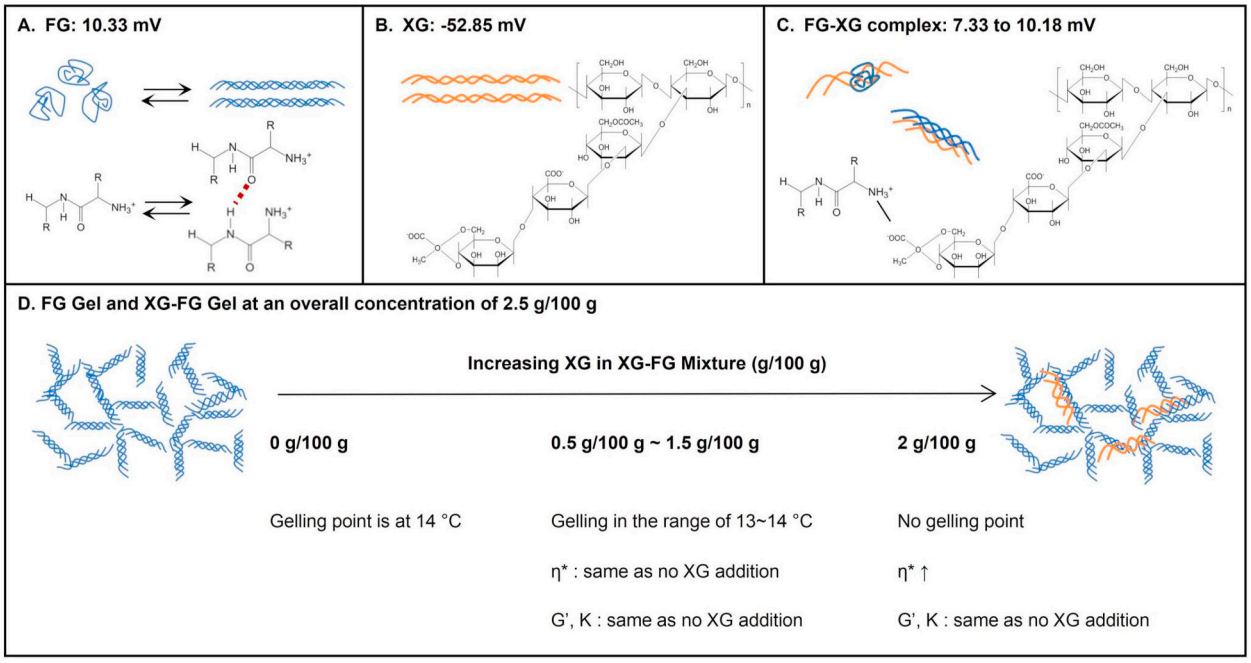

Fig. 2. Schematic diagram illustrating the (A) fish gelatin (FG), (B) xanthan gum (XG), (C) the xanthan gum-fish gelatin (XG-FG) complex formed by electrostatic interaction, and (D) the gelling properties of XG-FG with increasing XG:FG (w/w).

Walstra (1997) found that 0.01 g/100 g XG could contribute to the formation of the casein network. Under the same measurement parameters as this study, Pang, Deeth, and Bansal (2015) also found an increase in the G′ value ′ in a milk gel with 0.01 g/100 g XG addition during acidification. Previous studies by Wang et al. (2016), Pang et al. (2014) and Lucey, Van Vliet, Grolle, Geurts, and Walstra (1997) also proved that a synergistic gelling effect existed between XG and milk proteins.

Fig. 3 illustrates the representative rheological results and schematic models of XG-FG acid milk gels during the four stages (acidification, cooling, annealing, and heating). The schematic models are based on the models given by Cho, Lucey, and Singh (1999), Creamer et al. (1998), Syrbe, Bauer, and Klostermeyer (1998), and Tromp, de Kruif, van Eijk, and Rolin (2004).

During acidification (Fig. 3A), the primary gelling agent that caused an increase in the G′ value was the formation of casein network in milk (Pang et al., 2017). During cooling (Fig. 3B), the low temperature led to a decreased number or strength of hydrophobic bonds inside the casein particles, which caused swelling of the casein particles, and an increase in the G′ value (Pang et al., 2017). Moreover, low temperature caused FG to change into the helix form, which also contributed to the increase in the G′ value. During annealing (Fig. 3C), the G′ value of the gels did not change much with increasing time (Table 2), indicating that no obvious further gel-forming occurred. During heating (Fig. 3D), the G′ value of all samples decreased rapidly. Besides the melting of FG, shrinkage of the casein particles also caused this decrease (Lucey et al., 1997). The final the G′ value of all samples were similar at the end of this stage, as a result of the deformation of the gel network.

3.2.3. *Yogurt*

Previous research indicated that a XG:FG ratio of 1:99 could best mimic the rheological value of PG in the acid milk gel. Therefore, yogurt samples with a XG:FG ratio of 1:99 and an overall concentration of 0.4 g/100 g were studied. The addition of 0.4 g/100 g of gelatin in yogurt was within the concentration range (0.3–0.6 g/100 g) that was usually applied in yogurt production in previous studies (Ares et al., 2007; Luo et al., 2019; Pang et al., 2017). Yogurt with 0.4 g/100 g PG was included for comparison.

Fig. 4A shows the flow curves of yogurts with shear rate plotted versus shear stress. All samples showed hysteresis loops and thixotropic behavior. A higher shear stress value under the same shear rate represents a stronger gel structure with higher resistance to shear forces (Ares et al., 2007). The yogurts with PG (PY) and yogurts with XG-FG (XFY) had similar and higher shear stress values than yogurts with FG (FY) under shear rates from 0 to 100 s^{-1}, indicating a stronger gel structure in PY and XFY than in FY. Moreover, with an increasing shear rate, the difference in shear stress between FY and XFY increased. This indicated greater structural damage in FY at higher shear rates, whereas XFY was more stable under shear forces.

The upward curves in Fig. 4A were fitted to the Herschel-Bulkley model, and the results are shown in Table 3. The yield stress was zero in all samples, indicating that FY, XFY, and PY all flowed easily without

Table 2
Storage modulus (G′) of acid milk gels at the end of each stage during the dynamic oscillatory measurements. Values are presented as the mean ± SD.

Gelatin type	XG:FG	Storage modulus at the end of each stage (Pa)			
		Acidification	Cooling	Annealing	Heating
FG	0:100	379.5 ± 14.6^{c}	1751.2 ± 2.2^{c}	1827.7 ± 16.8^{c}	391.7 ± 19.8^{c}
	1:99	417.4 ± 34.1^{bc}	1923.2 ± 79.8^{bc}	2071.5 ± 63.1^{b}	420.7 ± 14.7^{bc}
	1.5:98.5	587.6 ± 6.7^{a}	2763.6 ± 95.1^{a}	2890.3 ± 8.5^{a}	610.5 ± 10.9^{a}
PG	–	466.5 ± 16.1^{b}	2138.1 ± 135.4^{b}	2165.1 ± 36.8^{b}	467.1 ± 11.8^{b}

[a-c] Mean values within a column and within a gel type with different letters are significantly different ($P < 0.05$).
*FG: fish gelatin, XG: xanthan gum, PG: pork gelatin.

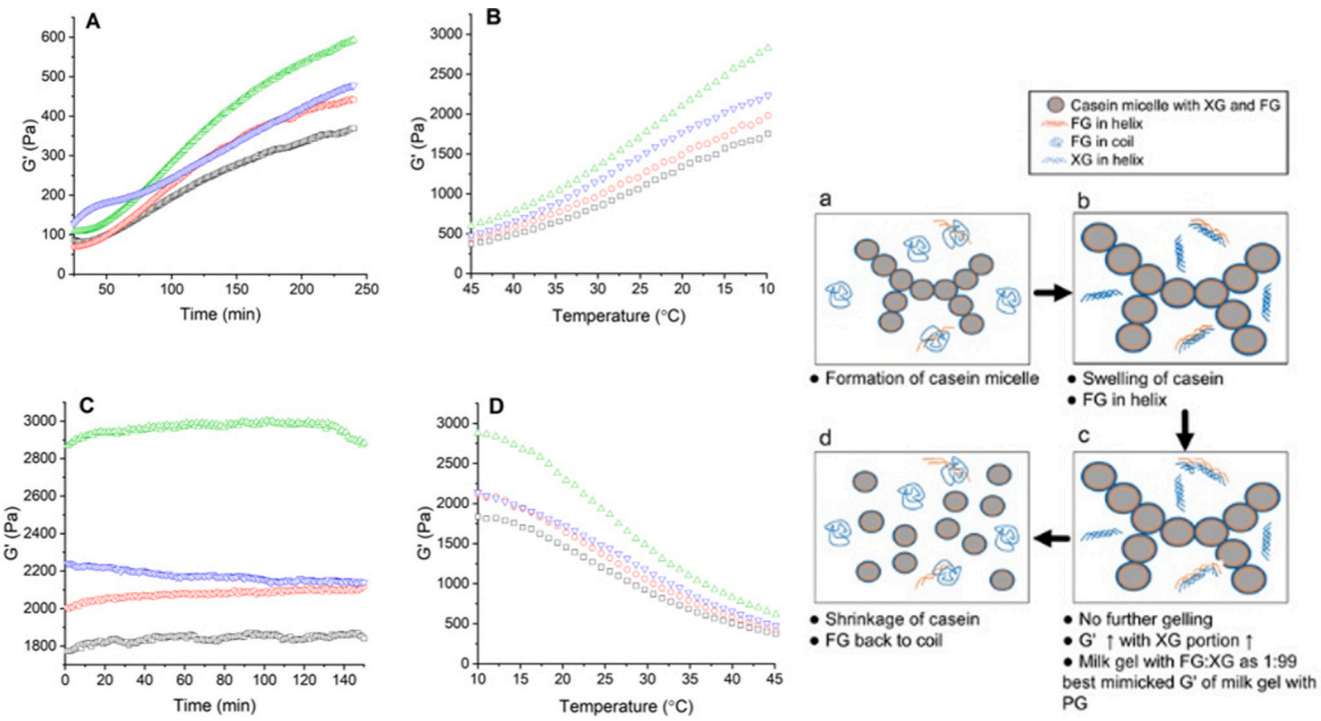

Fig. 3. Changes in storage modulus (G′) in acid milk gels with fish gelatin (FG), xanthan gum (XG)-FG at ratios of 99:1 (FX1) and 98.5:1.5 (FX1.5), and pork gelatin (PG) and the gelling schematic diagram during the process. (A,a) Acidification at 45 °C; (B,b) cooling from 45 to 10 °C; (C,c) annealing at 10 °C; and (D,d) heating from 10 to 45 °C. □, G′ of FG; ○, G′ of FX1; △, G′ of FX1.5; ▽, G′ of PG. Images a-d indicate schematic diagrams of each step, respectively.

a certain level of shear stress. Moreover, FY had a higher consistency coefficient (K) than PY. Similarly, Pang et al. (2017) found that FY had a lower K value than that of BY (yogurt with bovine gelatin). The addition of XG slightly decreased the K value of FY. Flow indexes (n) were similar in PY and XFY, and both of them were higher than that of FY, indicating that the addition of XG increased the pseudoplastic behavior of FY. The area of the hysteresis loop (ΔA) indicated structural breakdown and rebuilding with shearing (thixotropy). XFY had a higher ΔA value than FY. This indicated that compared with FY, XFY was less susceptible to structural breakdown during shearing, and more easily restructured the protein aggregates after shearing (Amatayakul, Halmos, Sherkat, & Shah, 2006; Ares et al., 2007).

Fig. 4B shows the changes in the G′ and G″ values in yogurt samples as a result of frequency change. All yogurts exhibited viscoelastic characteristics in the frequency sweep. The slope of the G′ plot was observed to be higher for XFY and PY than FY (Table 3), indicating a more frequency-dependent G′ value; and the slope of the G″ plot was lower for XFY and PY than for FY, indicating that the G″ value was more frequency-dependent in FY than PY and XFY. Similar relationships were shown between BY and FY (Pang et al., 2017). According to Pang et al. (2017), the moduli at a frequency (ω) of 1 Hz are shown in Table 3. XFY and PY had similar G′ and G″ values and were higher than those of FY, indicating a stronger yogurt gel structure was formed in XFY and PY, which was in accordance with the conclusions obtained by the acid milk gel test. The loss tangent (δ) values in Table 3 showed that the XFY and PY yogurts were more viscous in than FY.

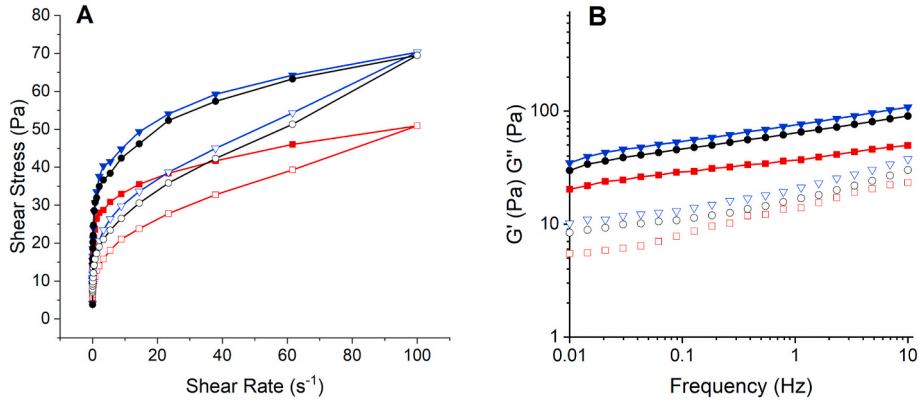

Fig. 4. (A) Flow curves of yogurt with shear rate first increasing (up) and then decreasing (down); FY: yogurt with fish gelatin, XFY: yogurt with fish gelatin and xanthan gum, PY: yogurt with pork gelatin. ■, FY-up; □, FY-down; ●, XFY-up; ○, XFY-down; ▼, PY-up; ▽, PY-down. (B) Frequency sweeps of yogurt from 0.01 to 10 Hz. G′: storage modulus, G″: loss modulus. ■, FY-G′; □, FY-G″; ●, XFY-G′; ○, XFY-G″; ▼, PY-G′; ▽, PY-G″.

Table 3
Rheological, viscoelastic, texture, and water-holding parameters of yogurts. Values are presented as the mean ± SD.

Test Type	Parameter	Sample Name		
		FY	XFY	PY
Flow Curves	Yield stress, σ_0 (Pa)	0.00 ± 0.00^{a}	0.00 ± 0.00^{a}	0.00 ± 0.00^{a}
	Consistency Coefficient, K ($Pa{\cdot}s^n$)	23.29 ± 0.91^{b}	29.05 ± 1.75^{a}	29.82 ± 2.40^{a}
	Flow behavior index (n)	0.17 ± 0.01^{b}	0.19 ± 0.01^{a}	0.19 ± 0.01^{a}
	Area under up-curve, A_{up} (s^{-1} Pa)	4261.06 ± 122.07^{b}	5787.78 ± 110.92^{a}	5942.66 ± 112.92^{a}
	Area difference ΔA	733.71 ± 38.30^{c}	1193.06 ± 106.10^{a}	1054.13 ± 38.73^{b}
Frequency Sweeps	G′, at 1 Hz	37.07 ± 2.77^{c}	65.4 ± 3.69^{b}	76.74 ± 7.68^{a}
	G″, at 1 Hz	4.59 ± 0.35^{c}	16.93 ± 1.58^{b}	21.08 ± 1.94^{a}
	Lost tangent δ, at 1 Hz	0.12 ± 0.01^{c}	0.26 ± 0.01^{b}	0.28 ± 0.02^{a}
	Slope of log (G′) vs. frequency	0.12 ± 0.00^{b}	0.15 ± 0.00^{a}	0.15 ± 0.01^{a}
	Slope of log (G″) vs. frequency	0.23 ± 0.03^{b}	0.18 ± 0.01^{a}	0.19 ± 0.01^{a}
Texture Analysis	Firmness (g)	30.89 ± 0.29^{b}	33.57 ± 0.83^{a}	32.29 ± 1.06^{a}
	Consistency (g·s)	210.51 ± 1.18^{c}	225.70 ± 2.92^{a}	217.77 ± 3.40^{b}
	Cohesiveness (g)	-15.54 ± 0.25^{b}	-20.69 ± 0.41^{a}	-19.53 ± 0.27^{a}
Water-Holding Capacity	WHC (%)	97.08 ± 0.21^{b}	100.00 ± 0.00^{a}	98.46 ± 0.04^{b}

[a-c] Means within a row with different letters are significantly different ($P < 0.05$).
XY: yogurt with fish gelatin; XFY: yogurt with fish gelatin and xanthan gum; PY: yogurt with pork gelatin.
*R^2 for the fitting of the flow curves results to Eq. (2) for all the samples were greater than 0.97. Mean squared error (MSE) for the fitting of the flow curves results to Eq. (2) for all the samples were less than 14.73.

3.3. Quality related analysis of yogurt

Whey expulsion as a result of spontaneous syneresis is a major parameter in the evaluation of yogurt quality. It happens because of the rearrangement of the gel network and the expelling of moisture during storage (Lucey, 2001). WHC measures the water-holding ability of yogurt and its stability from whey expulsion. Table 3 shows the WHC results of XFY, FY, and PY. PY had a similar WHC to FY, which agreed with the results of Shakila, Jeevithan, Varatharajakumar, Jeyasekaran, and Sukumar (2012), who found that the FG and PG had nearly the same WHC. No whey separation occurred in the XFY. This result indicated that XG could help to decrease whey separation in yogurt.

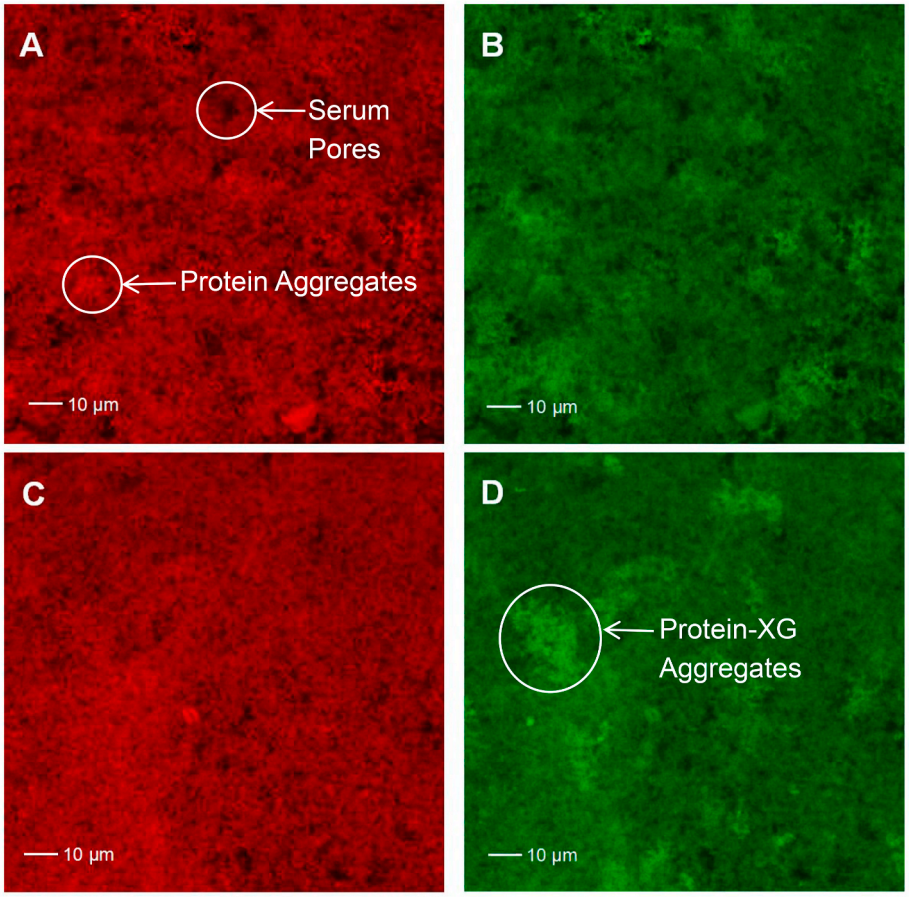

Fig. 5. Microstructure of yogurt with fish gelatin (FY, A and B), and yogurt with the mixture of fish gelatin and xanthan gum (XFY, C and D). *Rhodamine B stained proteins (red), while fluorescein isothiocyanate (FITC, green) stained polysaccharides and proteins.

Texture is another essential parameter to evaluate yogurt properties as it directly influences sensory perception by consumers. As a stabilizer, Gelatin is commonly used to modify the texture (Paseephol, Small, & Sherkat, 2008). Table 3 shows the texture results of FY, XFY, and PY. The addition of XG increased the firmness of the yogurt compared with that of FG ($P < 0.05$) and achieved a similar value to that of PY, which correlated with the results of the rheology test. Moreover, the consistency of the yogurt samples was also significantly increased by the addition of XG. From Table 3, the cohesiveness of XFY and PY were similar, and both were significantly higher than that of FY. Thus, the inner structures of XFY and PY were stronger than that of FY, which was as predicted from the results obtained in the rheology test.

The average results from two independent yogurt evaluation sessions are presented as spider diagram Figure S1. From the results, FY, XFY and PY had similar sense of melting. The homogeneity, thickness, and stickiness of the three samples were also comparable. And they had similar aroma without any weird smell. However, a slight increase was shown in thickness and stickiness scores with the addition of XG in yogurt, from 2.13 to 2.63, and 2.30 to 2.77, respectively ($P < 0.05$). The results were in accordance with the texture analysis.

3.4. Microstructure of yogurt

CLSM was used to observe the FY and XFY and illustrate the influence of XG on the microstructure of yogurt with FG (Fig. 5). Rhodamine B stained proteins in the yogurt samples with red color (Fig. 5A and C). Denser protein aggregates appeared in a lighter color, and the black areas represented serum pores (Dai et al., 2016). From Fig. 5A and C, XFY showed a homogeneous structure with a uniform appearance, while FY had a non-uniform structure with some over-dense parts, which represented protein aggregates. This indicates a more uniform structure in XFY than in FY, which correlated with the consistency result of TPA. Moreover, the black areas of the FY, representing serum pores, were larger than those of XFY, which helped to explain the better WHC of XFY compared with that of FY.

FITC stains both proteins and polysaccharides with green color (Qiu, Zhao, & McClements, 2015). Fig. 5A and B were from one FY sample at the same position under different wavelengths. Similarly, Fig. 5C and D were from one XFY sample at the same position under different wavelengths. Therefore, the existence of polysaccharides can be observed by comparing 5A with 5B, 5C with 5D, respectively. We can see similar structure and density in Fig. 5A and B. However, comparing to Fig. 5C, some denser aggregates were observed in Fig. 5D, indicating the presence of XG. Li and Shah (2015) also observed denser aggregates in the fermented milk with polysaccharides extracted from *Pleurotus eryngii* compared with those in the fermented milk without polysaccharide addition.

4. Conclusions

The main objective of this study was to determine the influence of XG addition on the rheological properties of FG, and to evaluate the potential of XG-modified FG as a replacement for mammalian gelatin in acid milk gels and low-fat yogurt. At a total concentration of 2.5 g/100 g, XG (0.0125 g/100 g to 0.05 g/100 g) did not influence the value of the storage moduli of FG gels but impeded the gelation process of fish gelatin as the amount of added XG increased. Moreover, the stages during yogurt manufacturing and consumption were monitored using acid milk gels as model systems. A proportion of XG to FG of 1:99 best mimicked the storage moduli of PG in milk gels. The addition of XG resulted in a more homogeneous structure of the yogurt made with FG. Yogurt with XG-modified FG had a better WHC than yogurt made with PG. However, their viscosity, pseudoplasticity, and thixotropy were similar. We concluded that XG-modified FG could be a potential replacement for PG in low-fat stirred yogurt.

Declaration of competing interest

The authors declare that they have no known competing financial interests or personal relationships that could have appeared to influence the work reported in this paper.

CRediT authorship contribution statement

Mengdi Yin: Data curation, Formal analysis, Investigation, Methodology, Resources, Validation, Visualization, Writing original draft. **Dongying Yang:** Resources, Data curation, Formal analysis, Investigation. **Shaojuan Lai:** Conceptualization, Funding acquisition, Project administration, review & editing. **Hongshun Yang:** Conceptualization, Funding acquisition, Project administration, Supervision, Writing – review & editing.

Acknowledgements

This study was funded by Project 31471605 supported by NSFC, the Singapore Ministry of Education Academic Research Fund Tier 1 (R-160-000-A40-114), and an industry project supported by Zhengzhou Bellad Biotechnology Co., Ltd (R-160-000-B15-597).

Appendix A. Supplementary data

Supplementary data to this article can be found online at https://doi.org/10.1016/j.lwt.2021.111643.

References

Amatayakul, T., Halmos, A. L., Sherkat, F., & Shah, N. P. (2006). Physical characteristics of yoghurts made using exopolysaccharide-producing starter cultures and varying casein to whey protein ratios. *International Dairy Journal, 16*(1), 40–51. https://doi.org/10.1016/j.idairyj.2005.01.004

Andersen, A., Ibsen, C. J. S., & Birkedal, H. (2018). Influence of metal ions on the melting temperature, modulus, and gelation time of gelatin gels: Specific ion effects on hydrogel properties. *The Journal of Physical Chemistry B, 122*(43), 10062–10067. https://doi.org/10.1021/acs.jpcb.8b07658

Ares, G., Gonçalvez, D., Pérez, C., Reolón, G., Segura, N., Lema, P., et al. (2007). Influence of gelatin and starch on the instrumental and sensory texture of stirred yogurt. *International Journal of Dairy Technology, 60*(4), 263–269. https://doi.org/10.1111/j.1471-0307.2007.00346.x

Bergmann, D., Furth, G., & Mayer, C. (2008). Binding of bivalent cations by xanthan in aqueous solution. *International Journal of Biological Macromolecules, 43*(3), 245–251. https://doi.org/10.1016/j.ijbiomac.2008.06.001

Chivero, P., Gohtani, S., Yoshii, H., & Nakamura, A. (2015). Effect of xanthan and guar gums on the formation and stability of soy soluble polysaccharide oil-in-water emulsions. *Food Research International, 70*, 7–14. https://doi.org/10.1016/j.foodres.2015.01.025

Cho, Y., Lucey, J., & Singh, H. (1999). Rheological properties of acid milk gels as affected by the nature of the fat globule surface material and heat treatment of milk. *International Dairy Journal, 9*(8), 537–545. https://doi.org/10.1016/S0958-6946(99)00123-5

Creamer, L. K., Plowman, J. E., Liddell, M. J., Smith, M. H., & Hill, J. P. (1998). Micelle stability: κ-Casein structure and function. *Journal of Dairy Science, 81*(11), 3004–3012. https://doi.org/10.3168/jds.S0022-0302(98)75864-3

Dai, S., Corke, H., & Shah, N. P. (2016). Utilization of konjac glucomannan as a fat replacer in low-fat and skimmed yogurt. *Journal of Dairy Science, 99*(9), 7063–7074. https://doi.org/10.3168/jds.2016-11131

Derkach, S. R., Voron'ko, N. G., Maklakova, A. A., & Kondratyuk, Y. V. (2014). The rheological properties of gelatin gels containing κ-carrageenan. The role of polysaccharide. *Colloid Journal, 76*(2), 146–152. https://doi.org/10.1134/S1061933X14020021

Huang, T., Tu, Z. C., Wang, H., Shangguan, X., Zhang, L., Niu, P., et al. (2017). Promotion of foam properties of egg white protein by subcritical water pre-treatment and fish scales gelatin. *Colloids and Surfaces A: Physicochemical and Engineering Aspects, 512*, 171–177. https://doi.org/10.1016/j.colsurfa.2016.10.013

Jellouli, K., Balti, R., Bougatef, A., Hmidet, N., Barkia, A., & Nasri, M. (2011). Chemical composition and characteristics of skin gelatin from grey triggerfish (*Balistes capriscus*). *LWT-Food Science and Technology, 44*(9), 1965–1970. https://doi.org/10.1016/j.lwt.2011.05.005

Kamer, D. D. A., Palabiyik, I., Işık, N. O., Akyuz, F., Demirci, A. S., & Gumus, T. (2019). Effect of confectionery solutes on the rheological properties of fish (Oncorhynchus mykiss) gelatin. *LWT-Food Science and Technology, 101*, 499–505. https://doi.org/10.1016/j.lwt.2018.11.046

Karim, A., & Bhat, R. (2009). Fish gelatin: Properties, challenges, and prospects as an alternative to mammalian gelatins. *Food Hydrocolloids, 23*(3), 563–576. https://doi.org/10.1016/j.foodhyd.2008.07.002

Kaur, A., Kumar, K., & Dhaliwal, H. S. (2020). Physico-chemical characterization and utilization of finger millet (*Eleusine coracana* L.) cultivars for the preparation of biscuits. *Journal of Food Processing and Preservation, 44*(9), Article e14672. https://doi.org/10.1111/jfpp.14672

Laneuville, S. I., Turgeon, S. L., Sanchez, C., & Paquin, P. (2006). Gelation of native β-lactoglobulin induced by electrostatic attractive interaction with xanthan gum. *Langmuir, 22*(17), 7351–7357. https://doi.org/10.1021/la060149+

Li, S., & Shah, N. P. (2015). Effects of *Pleurotus eryngii* polysaccharides on bacterial growth, texture properties, proteolytic capacity, and angiotensin-I-converting enzyme-inhibitory activities of fermented milk. *Journal of Dairy Science, 98*(5), 2949–2961. https://doi.org/10.3168/jds.2014-9116

Lucey, J. A. (2001). The relationship between rheological parameters and whey separation in milk gels. *Food Hydrocolloids, 15*(4–6), 603–608. https://doi.org/10.1016/S0268-005X(01)00043-1

Lucey, J., Van Vliet, T., Grolle, K., Geurts, T., & Walstra, P. (1997). Properties of acid casein gels made by acidification with glucono-δ-lactone. 1. Rheological properties. *International Dairy Journal, 7*(6–7), 381–388. https://doi.org/10.1016/S0958-6946(97)00027-7

Luo, Y., Liu, X., & Pang, Z. (2019). Tribo-rheological properties of acid milk gels with different types of gelatin: Effect of concentration. *Journal of Dairy Science, 102*(9), 7849–7862. https://doi.org/10.3168/jds.2019-16305

Milas, M., Reed, W. F., & Printz, S. (1996). Conformations and flexibility of native and re-natured xanthan in aqueous solutions. *International Journal of Biological Macromolecules, 18*(3), 211–221. https://doi.org/10.1016/0141-8130(95)01080-7

Nguyen, P. T., Kravchuk, O., Bhandari, B., & Prakash, S. (2017). Effect of different hydrocolloids on texture, rheology, tribology and sensory perception of texture and mouthfeel of low-fat pot-set yoghurt. *Food Hydrocolloids, 72*, 90–104. https://doi.org/10.1016/j.foodhyd.2017.05.035

Pang, Z., Deeth, H., & Bansal, N. (2015). Effect of polysaccharides with different ionic charge on the rheological, microstructural and textural properties of acid milk gels. *Food Research International, 72*, 62–73. https://doi.org/10.1016/j.foodres.2015.02.009

Pang, Z., Deeth, H., Sharma, R., & Bansal, N. (2015). Effect of addition of gelatin on the rheological and microstructural properties of acid milk protein gels. *Food Hydrocolloids, 43*, 340–351. https://doi.org/10.1016/j.foodhyd.2014.06.005

Pang, Z., Deeth, H., Sopade, P., Sharma, R., & Bansal, N. (2014). Rheology, texture and microstructure of gelatin gels with and without milk proteins. *Food Hydrocolloids, 35*, 484–493. https://doi.org/10.1016/j.foodhyd.2013.07.007

Pang, Z., Deeth, H., Yang, H., Prakash, S., & Bansal, N. (2017). Evaluation of tilapia skin gelatin as a mammalian gelatin replacer in acid milk gels and low-fat stirred yogurt. *Journal of Dairy Science, 100*(5), 3436–3447. https://doi.org/10.3168/jds.2016-11881

Paseephol, T., Small, D. M., & Sherkat, F. (2008). Rheology and texture of set yogurt as affected by inulin addition. *Journal of Texture Studies, 39*(6), 617–634. https://doi.org/10.1111/j.1745-4603.2008.00161.x

Pelletier, E., Viebke, C., Meadows, J., & Williams, P. (2001). A rheological study of the order–disorder conformational transition of xanthan gum. *Biopolymers: Original Research on Biomolecules, 59*(5), 339–346. https://doi.org/10.1002/1097-0282(20011015)59:5<339::AID-BIP1031>3.0.CO;2-A

Qiu, C., Zhao, M., & McClements, D. J. (2015). Improving the stability of wheat protein-stabilized emulsions: Effect of pectin and xanthan gum addition. *Food Hydrocolloids, 43*, 377–387. https://doi.org/10.1016/j.foodhyd.2014.06.013

Shakila, R. J., Jeevithan, E., Varatharajakumar, A., Jeyasekaran, G., & Sukumar, D. (2012). Functional characterization of gelatin extracted from bones of red snapper and grouper in comparison with mammalian gelatin. *LWT-Food Science and Technology, 48*(1), 30–36. https://doi.org/10.1016/j.lwt.2012.03.007

Sha, X. M., Zhang, L. J., Tu, Z. C., Zhang, L. Z., Hu, Z. Z., Li, Z., & Xiao, H. (2018). The identification of three mammalian gelatins by liquid chromatography-high resolution mass spectrometry. *LWT-Food Science and Technology, 89*, 74–86. https://doi.org/10.1016/j.lwt.2017.10.001

Sopade, P., Halley, P., & Junming, L. (2004). Gelatinisation of starch in mixtures of sugars. I. Dynamic rheological properties and behaviours of starch–honey systems. *Journal of Food Engineering, 61*(3), 439–448. https://doi.org/10.1016/S0260-8774(03)00153-5

Sow, L. C., Chong, J. M. N., Liao, Q. X., & Yang, H. (2018). Effects of κ-carrageenan on the structure and rheological properties of fish gelatin. *Journal of Food Engineering, 239*, 92–103. https://doi.org/10.1016/j.jfoodeng.2018.05.035

Sow, L. C., Toh, N. Z. Y., Wong, C. W., & Yang, H. (2019). Combination of sodium alginate with tilapia fish gelatin for improved texture properties and nanostructure modification. *Food Hydrocolloids, 94*, 459–467. https://doi.org/10.1016/j.foodhyd.2019.03.041

Sow, L. C., & Yang, H. (2015). Effects of salt and sugar addition on the physicochemical properties and nanostructure of fish gelatin. *Food Hydrocolloids, 45*, 72–82. https://doi.org/10.1016/j.foodhyd.2014.10.021

Syrbe, A., Bauer, W., & Klostermeyer, H. (1998). Polymer science concepts in dairy systems—an overview of milk protein and food hydrocolloid interaction. *International Dairy Journal, 8*(3), 179–193. https://doi.org/10.1016/S0958-6946(98)00041-7

da Trindade Alfaro, A., Fonseca, G. G., & Prentice-Hernández, C. (2013). Enhancement of functional properties of wami tilapia (*Oreochromis urolepis hornorum*) skin gelatin at different pH values. *Food and Bioprocess Technology, 6*(8), 2118–2127. https://doi.org/10.1007/s11947-012-0859-9

Tromp, R. H., de Kruif, C. G., van Eijk, M., & Rolin, C. (2004). On the mechanism of stabilisation of acidified milk drinks by pectin. *Food Hydrocolloids, 18*(4), 565–572. https://doi.org/10.1016/j.foodhyd.2003.09.005

Wang, C. S., Natale, G., Virgilio, N., & Heuzey, M. C. (2016). Synergistic gelation of gelatin B with xanthan gum. *Food Hydrocolloids, 60*, 374–383. https://doi.org/10.1016/j.foodhyd.2016.03.043

Wu, M., Qu, J., Shen, Y., Dai, X., Wei, W., Shi, Z., et al. (2019). Gel properties of xanthan containing a single repeating unit with saturated pyruvate produced by an engineered *Xanthomonas campestris* CGMCC 15155. *Food Hydrocolloids, 87*, 747–757. https://doi.org/10.1016/j.foodhyd.2018.09.002